

## Experimental Comparison of Neutrino and Muon Velocities\*

J. Alspector and G. R. Kalbfleisch

*Brookhaven National Laboratory, Upton, New York 11973*

and

Neil Baggett and Earle C. Fowler

*Purdue University, West Lafayette, Indiana 47907*

and

B. C. Barish, A. Bodek, D. Buchholz,† F. J. Sciulli, E. J. Siskind, and L. Stutte

*California Institute of Technology, Pasadena, California 91125*

and

H. E. Fisk, G. Krafczyk, and D. L. Nease

*Fermi National Accelerator Laboratory, Batavia, Illinois 60510*

and

Orrin D. Fackler

*Rockefeller University, New York, New York 10021*

(Received 22 January 1976)

The velocities of neutrinos and muons originating from  $\pi^+$  and  $K^+$  decays have been compared using the California Institute of Technology-Fermilab detector in a narrow-band neutrino beam. A time-of-flight comparison between positive muons and neutrinos, as indicated by the final-state negative muons in neutrino interactions, yields  $|\beta_\nu - \beta_\mu| \leq 0.4 \times 10^{-3}$  (99% confidence level). We assume that  $|1 - \beta_\mu| < 10^{-5}$  for these muons.

In a Fermilab experiment to measure the ratio of the cross section for the neutrino from pion decay ( $\nu_\mu$ ) to that for the neutrino from kaon decay ( $\lambda_\mu$ ), we have found that these neutrinos at 25 and 75 GeV have velocities which differ from those of energetic muons penetrating the shielding by no more than 4 parts in  $10^4$  [99% confidence level (CL)]. Such muons have high momentum  $p_\mu$  and velocity  $\beta_\mu = p_\mu / (p_\mu^2 + m_\mu^2)^{1/2}$  (where  $m_\mu$  is the muon mass) with  $|1 - \beta_\mu| < 10^{-5}$ .<sup>1</sup> The precision of this measurement is not sufficient to improve the presently accepted limits on the neutrino mass, but it is the first direct measurement of

neutrino velocity. The upper limit<sup>2</sup> on the mass of  $\nu_\mu$  is  $1.15 \text{ MeV}/c^2$  and that of  $\lambda_\mu$  is  $0.65 \text{ MeV}/c^2$ . If neutrinos are massless, it is expected that they move at the speed of light. However, since neutrinos are so vastly different from other known particles, this expectation should be tested experimentally.<sup>3</sup>

The experiment used the Fermilab narrow-band neutrino beam<sup>4</sup> (see Fig. 1) formed from a sign-selected hadron beam of adjustable central momentum ( $\Delta p/p = 36\%$  full width at half-maximum). This beam was directed into a 345-m-long evacuated decay pipe in which pion and kaon  $\mu\nu$  de-

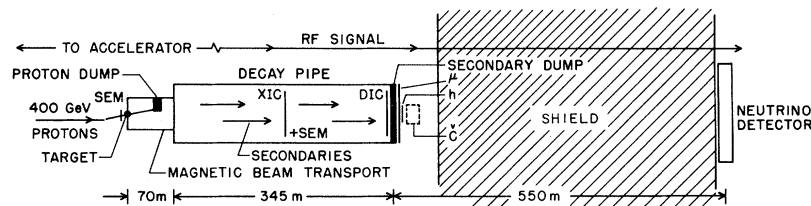


FIG. 1. A schematic drawing of the experimental layout. 400-GeV protons are incident on an Al target. Focusing and bending magnets form a sign- and momentum-selected parallel secondary beams of pions, kaons, and other particles. The neutrinos and muons are produced by decays of the pions and kaons as they traverse the 345-m evacuated decay pipe. Most hadrons are absorbed in the secondary dump. The neutrinos and a few energetic muons penetrate the 500-m earth and steel shield in front of the detector. SEM, XIC, DIG,  $\mu$ ,  $h$ , and  $\check{C}$  are monitors used in the cross-section experiment.

cays yielded a neutrino spectrum which, in the forward direction, contained two energy bands, the higher energy band from kaon decays and the lower one from pion decays.

Neutrino interactions such as  $\nu + \text{nucleon} \rightarrow \mu^- + \text{hadrons}$  were detected in a target calorimeter<sup>5</sup> located downstream behind 500 m of earth and steel shielding. The target contained seventy modules (each consisting of two 5-ft  $\times$  5-ft  $\times$  2-in. steel plates and a liquid-scintillator hadron-energy calorimetry counter) interspersed with 36 magnetostrictive-readout wire spark chambers, which monitored the muon trajectory through the target. A 5-ft-diam, 8-ft-long iron toroidal magnet followed by another twelve spark chambers was used to measure the muon momentum.

The apparatus was triggered by energy deposition in the calorimeter or by a muon traversing counters T3, T2, and T1 (see Fig. 2). A 10-ft  $\times$  10-ft counter plane normally vetoed incoming charged particles. However, a selected fraction of muons which penetrated the 500-m shield and the entire target were not vetoed. They were used to monitor counter calibration and to align spark chambers. The comparison of the time of flight of these muons with that of neutrinos, as indicated by the final-state muon from an interaction in the target, was made using counter T2.

Precise comparison of muon and neutrino velocities is possible because the 53.1-MHz radio-frequency accelerating system at Fermilab delivers protons to the production target in bunches about 1 nsec in duration and 18.83 nsec apart. Since pions and kaons at momenta  $\approx 80 \text{ GeV}/c$

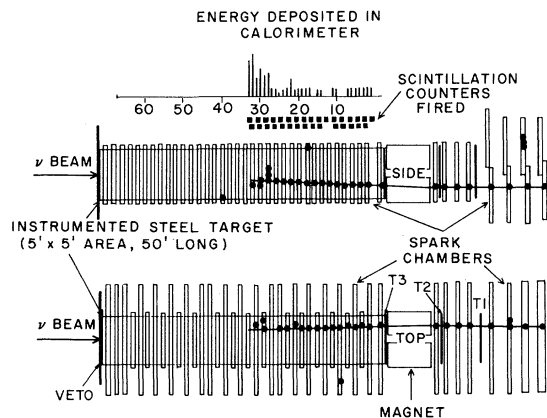


FIG. 2. An interaction of an 80-GeV neutrino in the target calorimeter. Note that the negative muons which are produced by neutrinos are focused as they pass through the iron toroidal magnet. Counter T2 is used for the neutrino-muon velocity comparison.

have velocity such that  $|1 - \beta_h| < 3 \times 10^{-5}$ , this time structure is retained by the secondary beam. Similarly, a muon from  $\pi$  or  $K$  decay remains in the same rf bunch as its parent, and those muons which penetrate the shield and detector should reproduce at T2 the original bunch size and spacing of the proton beam. This time structure is indeed observed for penetrating muons [see Fig. 3(a)].

If the neutrino velocity  $\beta_\nu$  differs sufficiently from unity, two effects would be expected. First, the neutrino bunches would be lengthened because hadron decays may occur anywhere along the 345-m decay pipe. For example, if  $\beta_h - \beta_\nu = +1.7 \times 10^{-2}$ , neutrinos from decays in one bunch at the upstream end would just overlap those from decays occurring in the next-following bunch as it reached the downstream end. This would cause the isolated peaks in the time spectrum to merge. Second, if  $\beta_\nu \neq \beta_\mu$ , the entire neutrino time spectrum would be shifted with respect to that of the muons.

As a reference for the timing measurement,

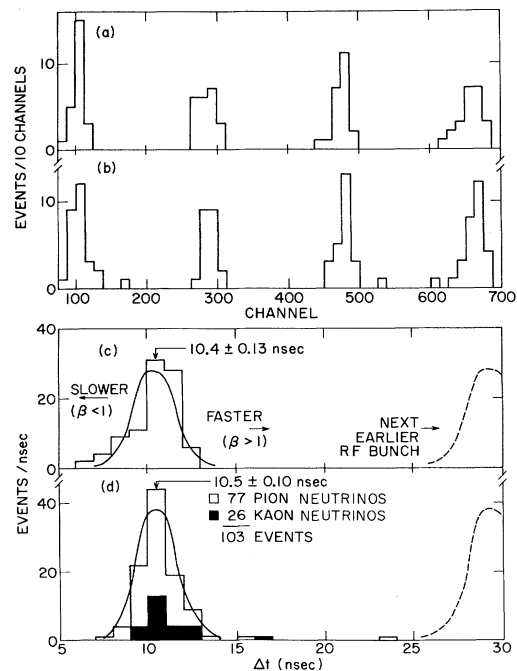


FIG. 3. T2-rf time spectra for selected muons traversing counter T2. (a) 250-GeV run, straight-through  $\mu^+$ , 91 events; (b) 80-GeV run,  $\mu^-$  from neutrino interactions, 103 events [there are four peaks in (a) and (b) because the rf pulse train used to stop the time-to-digital converters was prescaled by four]; (c) spectrum from (a) combined by displacement of appropriate multiples of 185 channels; (d) combined spectrum from (b).

the accelerator rf signal was zero-crossing discriminated and prescaled by four to yield a train of standard logic pulses spaced every 75.3 nsec or four rf bunches. Whenever there was an event in which both phototubes on counter  $T3$  counted, the time-averaged signal from these tubes was used to start simultaneously two time-to-digital converters (TDC's) with 100-psec resolution (Ortec TD 811). One of the TDC's was stopped by the time-averaged signal from the two phototubes on counter  $T2$ , while the other was stopped by the 75.3-nsec pulse train. The TDC data were recorded on tape after each event along with pulse-height information from the calorimetry counters and spark-chamber data. The time of the  $T2$  counter pulse relative to the rf pulse was extracted by subtracting the data from the two TDC's.

We report on runs taken with the narrow-band beam set to select 250 and 80-GeV positive secondaries. From the 250-GeV data, 91 straight-through muons were selected which traversed the target, magnet, and counters  $T3$  and  $T2$ . In addition, it was required that they be defocused by the toroid, thus indicating positive charge. Such particles have residual energies between 15 and 45 GeV on entering the target. These muons had to come from the decay pipe and not from neutrino interactions in the shield because such interactions produce  $\mu^-$ 's, while  $\mu^+$ 's are produced by  $\pi^+$  and  $K^+$  decays.

From the 80-GeV data, 103 neutrino events were selected in which the final-state  $\mu^-$  traversed the magnet and counters  $T3$  and  $T2$ . The interaction vertex was located between counters 12 and 67 and at least 5 in. from the edge of the target. Figures 3(a) and 3(b) illustrate that the muon and neutrino time spectra show the rf structure of the accelerator and that peaks occur in the same timing channels. There are three background events. At the present statistical level, these events are ignored in what follows. However, we note that if there are heavy leptons which produce muons via decays in flight or interactions in the target,<sup>6</sup> they could give rise to muons or neutrino-like events which would not show the same time structure as neutrino or muon events. After analyzing more data, we should be able to set quantitative limits on the production of such particles.

In order to quantify the velocity difference between muons and neutrinos, we use the difference in the mean position of the timing peaks. The means and rms deviations were determined for

the eight peaks in Figs. 3(a) and 3(b). The 185-channel mean separation of the peaks corresponds to the 18.83-nsec period between accelerator bunches. The observed rms deviation of 12 channels is consistent with the known resolving time of the  $T2$  time-averaged pulse and its associated electronics.<sup>7</sup> This sharpness of the peaks indicates that both  $\beta_\nu$  and  $\beta_\mu$  differ from  $\beta_h$  by less than  $2 \times 10^{-3}$ . Therefore the two spectra cannot have been shifted by even one bunch.

Each set of four peaks was combined by displacements of appropriate multiples of 185 channels [see Figs. 3(c) and 3(d)]. For the final comparison the scales were converted to nanoseconds. Normalized Gaussian curves with full widths at half-maximum of 2.8 nsec were drawn at the positions of the mean times along with dashed curves indicating the immediately preceding bunch (18.83 nsec later). The neutrino events were separated into those with total energy less than 50 GeV (77  $\nu_\mu$  events) and those with energy greater than 50 GeV (26  $\lambda_\mu$  events). No difference between the two groups was observed.

The time difference  $\Delta t$  between the muons and  $\nu_\mu$  events is  $0.05 \pm 0.19$  nsec; i.e.  $< 0.5$  nsec (99% CL). For the  $\lambda_\mu$  events, it is  $0.37 \pm 0.24$  nsec; i.e.  $< 1.0$  nsec (99% CL). The mean flight path to counter  $T2$  is taken to be  $550 + \frac{1}{2} \times 345$  m or 2400 nsec. Thus the final result is as follows: For 25-GeV neutrinos from pion decay,  $\nu_\mu$ ,

$$|\beta_\nu - \beta_\mu| \leq 0.2 \times 10^{-3} \text{ (99\% CL);}$$

for 75-GeV neutrinos from kaon decay,  $\lambda_\mu$ ,

$$|\beta_\lambda - \beta_\mu| \leq 0.4 \times 10^{-3} \text{ (99\% CL).}$$

We expect to continue this analysis in order to reduce statistical errors and to cover the entire energy range from 25 to 250 GeV more thoroughly.

It is a pleasure to acknowledge the support and hospitality of Fermilab and its staff, in particular J. Griffin, L. Beverley, R. Stefanski, R. Lundy, J. Sanford, and R. R. Wilson. Additional persons supplied significant help in carrying out this experiment. We especially want to thank K. W. Brown, R. Moyer, K. Nishikawa, M. Shaevitz, J. Lee, Y. K. Chu, P. Dishaw, and H. Kwon.

\*Work supported by the U. S. Energy Research and Development Administration.

†Permanent address: Northwestern University, Evanston, Ill. 60201.

<sup>1</sup>The relation  $\beta = p/(p^2 + m^2)^{1/2}$  has been confirmed experimentally for electrons for values of  $1 - \beta$  down to

$2 \times 10^{-7}$  [Z. G. T. Guiragossian *et al.*, Phys. Rev. Lett. **34**, 335 (1975). See also E. V. Schrum and K. O. H. Ziock, Phys. Lett. **37B**, 114 (1971); G. Backenstoss *et al.*, Phys. Lett. **43B**, 539 (1973); A. R. Clark *et al.*, Phys. Rev. D **9**, 533 (1974)]. We assume for this discussion that it holds for muons, pions, and kaons, with momentum up to 250 GeV/c.

<sup>2</sup>For  $\nu_\mu$ , see Schrum and Ziock, Ref. 1, and Backenstoss *et al.*, Ref. 1. For  $\lambda_\mu$ , see Clark *et al.*, Ref. 1.

<sup>3</sup>G. R. Kalbfleisch, BNL Informal Report No. 20227 (unpublished).

<sup>4</sup>B. C. Barish *et al.*, unpublished; P. Limon *et al.*, Nucl. Instrum. Methods **116**, 317 (1974).

<sup>5</sup>B. C. Barish *et al.*, Phys. Rev. Lett. **35**, 1316 (1975), and Nucl. Instrum. Methods **116**, 413 (1974).

<sup>6</sup>Recent publications discuss the existence of such leptons. See e.g., M. R. Krishnaswamy *et al.*, Phys. Lett. **57B**, 105 (1975); A. De Rújula *et al.*, Phys. Rev. Lett. **35**, 628 (1975); A. Benvenuti *et al.*, Phys. Rev. Lett. **35**, 1486 (1975).

<sup>7</sup>The total resolving time (full width at half-maximum) is made up of several contributions: (a) the 1-nsec spread of the rf bunch; (b) possible jitter in the rf signal and its electronics; (c) the  $2\frac{1}{2}$ -nsec intrinsic resolution of the two photomultipliers on either side of the counter T2; and (d) the  $\frac{1}{2}$ -nsec slewing of the time-averaged signal of the T2 photomultipliers. Cosmic rays were used to determine the correlation between particle position in T2 and the slewing of the time-averaged pulse.

## Theoretical Limits on Interstellar Magnetic Poles Set by Nearby Magnetic Fields

S. A. Bludman\*

*Department of Physics, University of Pennsylvania, Philadelphia, Pennsylvania 19174*

and

M. A. Ruderman†

*Department of Physics, Columbia University, New York, New York 10027*

(Received 26 January 1976)

The interstellar magnetic field limits the monopole flux to  $< 10^{-16}$  pole  $\text{cm}^{-2} \text{sec}^{-1}$  and gives the average monopole energy  $10^{11}$  GeV. They can be detected nonrelativistically only if their mass is  $\approx 10^{11}$  GeV/c<sup>2</sup> and, being produced at  $E > 10^{22}$  GeV, require  $10^{21}$  g  $\text{cm}^{-2}$  matter for ionization loss to make them nonrelativistic. Massive monopoles can only be primordial or cosmologically produced. Low-mass monopoles trapped in dust grains and released in the atmosphere are possible.

Magnetic monopoles were originally proposed<sup>1,2</sup> to explain the quantization of electric charge and to symmetrize Maxwell's equations between electric and magnetic currents. Recently, magnetic monopole solutions have been demonstrated in any unified non-Abelian gauge theory containing electromagnetism within a larger compact covering group.<sup>3</sup> In these theories, the monopole mass is

$$M = 137 M_w \geq 6000 \text{ GeV}/c^2, \quad (1)$$

where  $M_w$ , the mass of the vector meson, is about  $53 \text{ GeV}/c^2$  in the Georgi-Glashow O(3) theory, but is much larger in theories containing superheavy vector mesons.

The existence of any magnetic monopole may require profound alterations in our quantum field theoretic understanding of elementary particles. However, the analysis we are about to present depends only on classical electrodynamics which, because of the large pole mass and strong coup-

ling of monopoles,

$$g = 137e = 6.6 \times 10^{-8} \quad (2)$$

(in Gaussian cgs units), is adequate to describe their propagation and energy loss in matter. We note first that the persistence of interstellar magnetic fields in the Sun's neighborhood sets very low limits on the flux of any cosmically produced magnetic monopoles. Another consequence is that galactic- or extragalactic-produced monopoles would have average energies exceeding  $E \sim 10^{11}$  GeV; they could therefore be differentiated from high- $Z$  heavy nuclei by ionization loss only if their mass  $M \geq 10^{11}$  GeV. But such hugely massive particles would be produced with laboratory energies exceeding  $10^{22}$  GeV and would not become nonrelativistic in our present universe. In order for a monopole to reach Earth's atmosphere at slow velocity, it must have  $M > 10^{11} \text{ GeV}/c^2$  and be primordial or cosmological in origin, or have reached Earth's atmosphere inside an interstellar dust grain.